Scientific Research Publishing

Open Journal of Polymer Chemistry, 2024, 14, 19-40
https://www.scirp.org/journal/ojpchem
ISSN Online: 2165-6711
ISSN Print: 2165-6681

Preparation and Performance Study of PVA-Based Flexible Sensors

Md Kamrul Hasan, Xinbo Ding*

School of Textile Science and Engineering, International Silk Institute, Zhejiang Sci-Tech University, Hangzhou, China
Email: *dxblt@zstu.edu.cn

How to cite this paper: Hasan, M.K. and Ding, X.B. (2024) Preparation and Performance Study of PVA-Based Flexible Sensors. *Open Journal of Polymer Chemistry*, **14**, 19-40.
https://doi.org/10.4236/ojpchem.2024.141002

Received: January 19, 2024
Accepted: February 24, 2024
Published: February 27, 2024

Abstract

Flexible sensors have great potential for monitoring human body motion signals. This paper presents a flexible sensor that uses zinc oxide (ZnO) to improve the mechanical properties and electrical conductivity of PVA hydrogel. The composite hydrogel has excellent conductive properties and high strain sensitivity, making it suitable for motion monitoring. The PVA/ZnO conductive hydrogel is tested on various body parts, showing effective feedback on movement changes and good electrical signal output effects for different motion degrees, confirming its feasibility in flexible sensors. The sensor exhibits good mechanical properties, electrical conductivity, and tensile strain sensing performance, making it a promising sensor material. It can accurately monitor wrist bending, finger deformation, bending, and large-scale joint movements due to its wide monitoring range and recoverable strain. The results show that the PVA/ZnO conductive hydrogel can provide effective feedback in flexible sensors, which is suitable for use in motion monitoring.

Keywords

Polyvinyl Alcohol, Zinc Oxide, Zinc Oxide Nanorods, Conductive Hydrogel, Flexible Sensor

1. Introduction

Recently, the application of sensors has gradually become more and more widespread, and the scope of its application is also gradually expanding. External condition stimuli such as temperature [1], pressure [2] [3], strain [4], and humidity [5] [6] can convert the stimulus signal into an electrical signal through the sensor. Through the electrical signal feedback of the sensor, subtle changes can be sensed. Environmental changes enable sensors to have broad application

prospects in digital medicine [7] [8], bionic skin [9], smart devices [10], and user interaction [11]. Conductive hydrogels are excellent candidate materials for flexible sensors. Because hydrogels have excellent performance in tensile strength, tensile ductility, and biocompatibility, they have been widely reported in research [12] and attention. However, as a bionic electronic skin, the material maintains good mechanical properties and is able to provide timely feedback to external stimuli [13] to achieve a comprehensive simulation of human skin. Developing conductive wearable materials with both excellent mechanical properties and high resistance sensitivity still faces severe challenges [14]. Polyvinyl alcohol (PVA) is a widely used water-soluble polymer composed of polyvinyl acetate. It exhibits high reactivity with various functional groups, high water affinity, processability, and minimal cell and protein adhesion [15] [16] [17] [18]. PVA was first produced in 1924 by German scientists W.O Hermann and W. Haehne. PVA can be prepared chemically or physically to produce hydrogels, with the freeze-thaw (F-T) process being the most commonly used. Its unique properties include film-forming, adhesive, biocompatibility, high strength, swelling, safety, and adhesive properties, making it widely used in industry, agriculture, and medicine. However, PVA has major shortcomings, such as swelling characteristics affecting stability in open environments and different crystallization properties due to reorganization. Compounding and modification of materials can improve their mechanical properties and functionality, expanding their applications. This compatibility allows for more methods for physical and chemical modification, making PVA more suitable for flexible hydrogel sensors [19]. Zinc oxide, a broadband n-type semiconductor oxide, has a band gap of 3.2 eV and a laser binding energy of up to 60 meV. It has three crystal structures: salt rock, sphalerite, and hexagonal wurtzite. It is an environmentally friendly nanomaterial with great development potential. The hexagonal wurtzite structure has relatively stable thermodynamic properties. Zinc oxide has applications in antibacterial materials, photocatalytic materials, rubber materials, and sensors [20] [21]. Zinc oxide is a crucial antibacterial material, with various mechanisms including photocatalytic, zinc ion dissolution, and contact adsorption [22]. The smaller the particle size, the larger the specific surface area, and the greater the contact reaction area with bacteria [23]. Studies show that nano-zinc oxide has a strong inhibitory effect on Escherichia coli and Staphylococcus aureus [24]. The hydrophilicity and swelling properties of the chitosan/silk cellulose/zinc oxide nanocomposite prepared by Salama [25] have been significantly improved, demonstrating broad antibacterial activity. Semiconductor heterogeneous photocatalysis, a green technology using advanced oxidation processes, is gaining recognition for wastewater remediation and water purification due to its nontoxicity and high stability [26]. Zinc oxide enhances rubber vulcanization, improving its mechanical properties [27]. Over 50% are used in tire production. Zhang *et al.* [28] improved adhesion between nanowires and silane-grafted fiber. Sensors are devices that convert measured objects into usable output signals. Zinc oxide,

due to its high chemical sensitivity, non-toxicity, and low cost, is widely used in biosensors, gas sensors, piezoelectric materials, and varistors [29] [30]. A flexible sensor on a Kapton substrate is fabricated using polydimethylsiloxane/zinc oxide nanowires, with a sensitivity of 23.6 mV/kPa [31]. Hydrogels are classified by preparation method, charge, and structural properties. They can be amorphous, semi-crystalline, hydrogen-bonded, membrane, or hydrocolloid [32]. They can be made from natural or synthetic polymers, with a combination of both being popular in biomedical applications [33]. Conductive hydrogels are modified and improved by introducing different conductive polymers to meet the conductivity requirements of flexible sensor materials. The main conductive filling materials include conductive polymers [34], carbon-based materials [35], MXenes [36], wall carbon nanotubes [37], and ionic materials. These materials are widely used in flexible conductive hydrogel materials due to their excellent electrical properties and stability. Meanwhile, when preparing the sensing substrate, the transmission path is improved by improving the three-dimensional microscopic pores. Controlling the doping amount of conductive fillers can balance the mechanical and conductive properties of the material. Flexible hydrogel materials constructed from conductive polymers are also widely used as sensor substrates due to their simplicity in conductivity control and synthesis. The rigid molecular chain and hydrophobic properties of conductive polymers can destroy the hydrogel's toughness. Conductive and mechanical properties can be improved by using highly functionalized graphene oxide. MXene-based hydrogels exhibit low tensile strength and tensile strain capacity due to the lack of a three-dimensional network skeleton [38]. Metal-based hydrogel sensors use the softness [39] and strain properties of liquid metal to provide feedback effects on the external environment [40]. This hydrogel sensor, by providing feedback on knuckle frequency and bending angle, can effectively monitor the movement of the finger joint. It is suitable for monitoring changes such as elbow and knee movements and can also provide accurate results for large-scale movement of moving joints. Overall, this PVA/ZnO conductive hydrogel sensor shows excellent sensing performance and can be used to detect human body motion signals, and the results are quite satisfactory for detecting human body motion signals.

2. Experimental Section

2.1. Experimental Materials

Polyvinyl alcohol (PVA1799, n = 1700, degree of alcoholysis 99%), and zinc acetate dihydrate $Zn(CH_3COO)_2{\cdot}2H_2O$ are purchased from Shanghai Macklin Biochemical Technology. All reagents are used in their original form. Deionized water (DIW) is used, which is made in the laboratory.

2.2. Preparation of ZnO

Pure ZnO nanorods are prepared through a mechanically assisted thermal decomposition process. During the synthesis of zinc oxide nanorods, 20 g of zinc

acetate dihydrate [$Zn(CH_3COO)_2{\cdot}2H_2O$] is ground in a mortar for 45 min. The ground powder is placed in an alumina crucible, the heating rate is set to 4˚C/min, the temperature is raised to 300˚C, and the heating is continued in a muffle furnace for 4 h. The obtained powder is then washed with deionized water, washed twice, and then dried in an oven at 100˚C for 10 h to finally obtain zinc oxide nanorods.

2.3. Preparation of PVA/ZnO Conductive Hydrogel

6 g of PVA and 54 mL of deionized water are added to a beaker and stirred at 45˚C for 30 min, and then the temperature is raised to 95˚C to fully dissolve PVA for 2 h to obtain a homogeneous and transparent aqueous solution of PVA with 10 wt%. After the solution is cooled, different mass ratios of zinc oxide are added, and the zinc oxide is uniformly dispersed in the PVA solution by ultrasonic stirring. The resulting solution is then injected into a 40 mm × 10 mm × 1 mm mold. The solution is stored at −5˚C for 14 h by the freeze-thaw method to completely freeze the solution, and then thawed at room temperature for 6 h and cycled three times to obtain the PVA/ZnO conductive hydrogel. Are named PZ0, PZ0.1, PZ0.4, PZ0.8, and PZ1.2. The subscript represents the mass percentage of ZnO.

2.4. Characterization

The PHP1 surface morphology is examined using an Ultra55 field emission scanning electron microscope (FE-SEM). Freeze-dried samples are putter-coated with platinum for 100 seconds before being observed under a 3 kV accelerating voltage. ATR-FTIR spectra of hydrogels are obtained on a Nicolet IS50 Fourier Transform Infrared (FTIR) spectrometer in the wavelength region of 400 - 4000 cm^{-1}. A D8 Discover X-ray diffractometer is used to examine the samples for wide-angle crystal structure scanning analysis. The sample is calibrated in a chamber with a voltage of 40 kV, a current of 40 mA, and a radiation source of Cu target Kα rays, with a scanning range of 5˚ - 80˚ and a scanning step of 5˚/min.

2.5. Mechanical Testing

The tensile mechanical properties of conductive hydrogels are determined using the Instron5969 universal testing machine under the clamping of tensile strength tester. The sample size is 10 mm × 5 mm × 1 mm, the clamping distance is 10 mm, and the stretching speed is 1 mm/min. The calculation formula for tensile stress is:

$$\sigma_{stress} = F/A_0 \tag{2-1}$$

In the formula: σ_{stress}: Stress in hydrogels, kPa; F: The tension exerted by the hydrogel, N; A_0: The cross-sectional area of the hydrogel, m^2.

2.6. Electrical Measurements Testing

A Keithley 2400 digital source meter with a dual-electrode system is used to

measure conductivity. A Keithley 2400 digital source meter is connected to a copper wire with conductive electrodes attached to both ends of a 40 mm × 10 mm × 1 mm hydrogel material. The resistance of the hydrogel material is obtained by linearly scanning the voltammetry curve and the conductivity of the hydrogel material is calculated using the formula (2-2):

$$\sigma_{\text{Conductivity}} = L/RS \tag{2-2}$$

In the formula: $\sigma_{\text{Conductivity}}$: The conductivity of the hydrogel, S/m; R: Volume resistance of hydrogel, Ω; L: the length of the hydrogel, m; S: The cross-sectional area of the hydrogel, m^2.

The strain sensor performance of the conductive hydrogel is tested using a Keithley 2400 digital source meter and an electric tensile testing machine. A conductive hydrogel sample of 10 mm × 5 mm × 1 mm is fixed in the fixture of the electric tensile testing machine and connected to both ends of the digital source meter through wires to test the resistance change of the material during the change of movement. Determine the relative resistance change rate by doing the following:

$$\text{Relative resistance change rate} = (R - R_0)/R_0 * 100\% \tag{2-3}$$

where: R: the resistance of the hydrogel during stretching, Ω; R_0: The initial resistance of the hydrogel when it is not stretched, Ω.

2.7. Sensitivity Factor

The measurement factor (GF) of hydrogel sensitivity is obtained by the following formula:

$$\text{GF} = (R/R_0)/\varepsilon \tag{2-4}$$

In the formula: ε: represents the applied strain, %; $\Delta R/R_0$: Relative resistance change rate, %.

3. Results and Discussion

3.1. Structural Characterization of ZnO

1) Field emission scanning electron microscope (FE-SEM)

As can be seen from the SEM image of zinc oxide nanorods in Figure 1 below, the zinc oxide nanorods are arranged in a disorderly manner. It can be seen from the particle size distribution diagram of zinc oxide nanorods in Figure 2 that the particle size range of zinc oxide nanorods is concentrated between 50 and 65 nm.

2) EDS of zinc oxide

The EDS spectrum of zinc oxide is shown in Figure 3. The characteristic peaks of zinc oxide are detected at 0.52 KeV and 1.02 KeV, respectively, which are O and Zn elements, respectively, and the weight percentages of O and Zn elements are 18.45% and 81.55%, respectively. This indicates the successful preparation of zinc oxide.

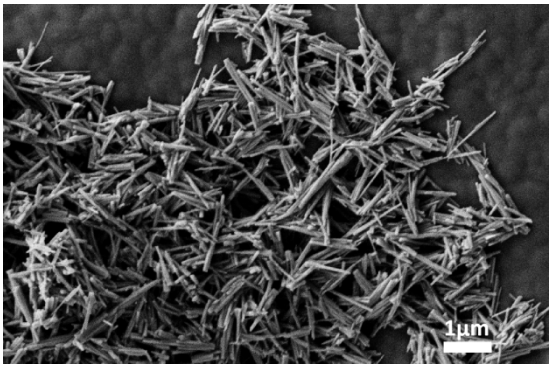

Figure 1. Electron microscope morphology of **ZnO**.

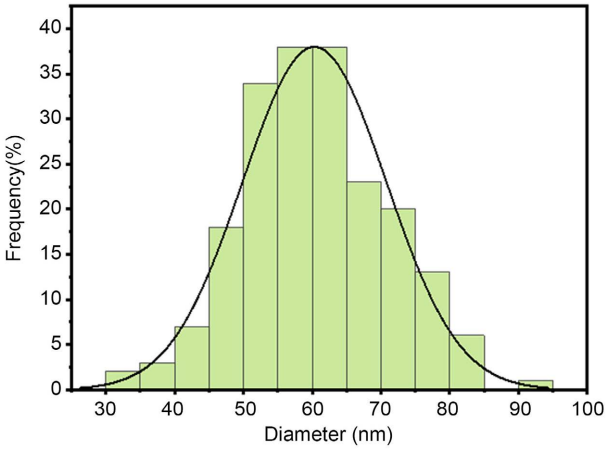

Figure 2. Diameter distribution diagram of **ZnO**.

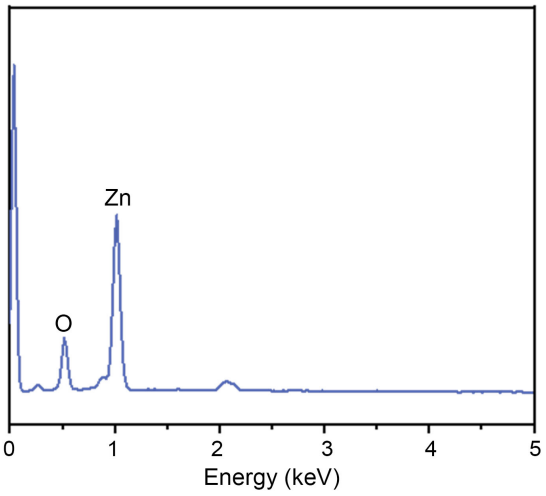

Figure 3. EDS of zinc oxide.

3) Fourier transform infrared spectroscopy (FTIR)

Figure 4 shows the infrared spectrum of zinc oxide. The absorption peak at 501 cm^{-1} is a typical characteristic absorption peak of wurtzite hexagonal phase pure zinc oxide. The characteristic absorption peak of zinc oxide proves the successful preparation of zinc oxide.

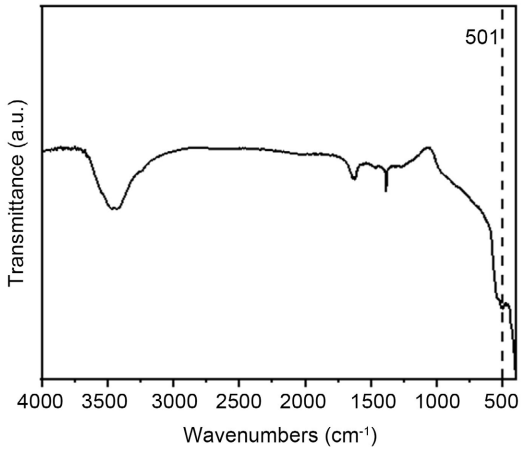

Figure 4. Infrared spectrum of zinc oxide.

4) X-ray diffraction spectrum analysis (XRD)

XRD patterns are used to evaluate the crystal structure of zinc oxide. As shown in **Figure 5**, the diffraction peaks appearing at $2\theta = 31.85$, 34.48˚, 36.30˚, 47.57˚, and 56.63˚ correspond to the (100), (002), (101), (102), and (110) planes. These peaks show the crystallographic faces of the typical wurtzite (hexagonal) structure of ZnO nanoparticles (JCPDS card number 36-1451) [41].

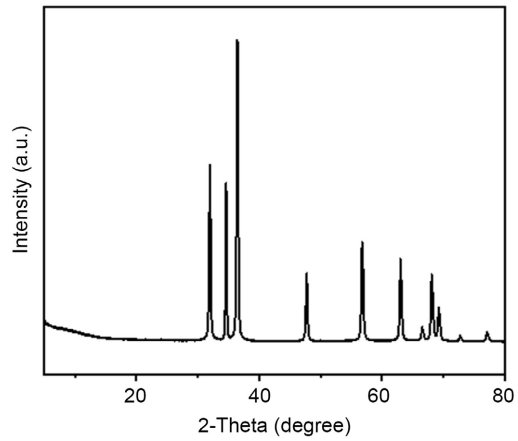

Figure 5. XRD of zinc oxide.

3.2. Characterization of Structural Properties of PVA/ZnO Conductive Hydrogel

1) Field emission scanning electron microscope (FE-SEM)

It can be seen from **Figure 6** that after the introduction of zinc oxide, the three-dimensional network structure of the hydrogel is obvious in the field emission scanning electron microscope pattern, and the pore size is almost evenly distributed. Moreover, zinc oxide nanorods are evenly distributed and interspersed between the three-dimensional network of the hydrogel. The PVA/ZnO conductive hydrogel has a unified three-dimensional network, which is also conducive to the rapid transmission of electrical signals.

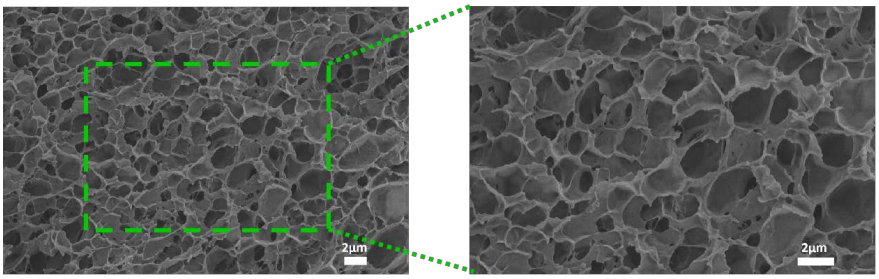

Figure 6. Microscopic morphology of PVA/ZnO conductive hydrogel.

2) EDS and element distribution diagram of PVA/ZnO conductive hydrogel

Figure 7 shows the EDS and elemental distribution diagrams of PVA/ZnO conductive hydrogel. In addition to the common C and O elements in polyvinyl alcohol hydrogels, Zn elements also appear in PVA/ZnO conductive hydrogels, which is attributed to the presence of oxidation and further demonstrates the presence of zinc oxide in the blending method. There is a certain interaction with polyvinyl alcohol hydrogel. It can be seen from the element distribution diagram corresponding to the conductive hydrogel that the Zn element is evenly distributed in the hydrogel, which shows that zinc oxide and polyvinyl alcohol can be evenly mixed together.

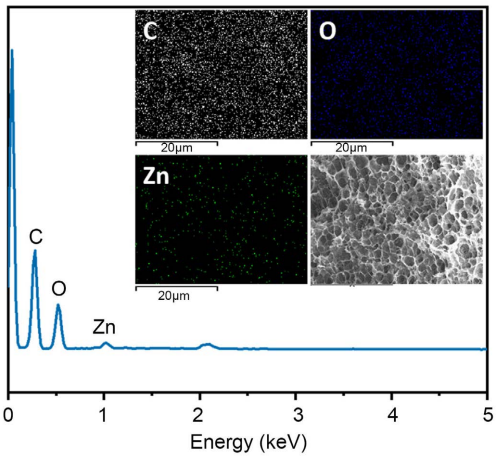

Figure 7. EDS and element distribution diagram of PVA/ZnO conductive hydrogel.

3) Fourier transform infrared spectroscopy (FTIR)

In order to evaluate the interaction between zinc oxide and polyvinyl alcohol, infrared spectral analysis is performed on polyvinyl alcohol and polyvinyl alcohol/zinc oxide composite hydrogels. The spectra are shown in Figure 8. The characteristic peak at 3264 cm^{-1} is the -OH characteristic absorption peak, which shifts to 3248 cm^{-1} on the PZ hydrogel, which is the strong interaction between polyvinyl alcohol and the hydroxyl groups in zinc oxide. The peak at 2937 cm^{-1} represents the stretching vibration peak of C-H2 in PVA, which is the hydrophobic main chain structure of polyvinyl alcohol; the peak at 1658 cm^{-1} is the -OH deformation vibration peak. 501 cm^{-1} is the Zn–O vibration peak. The

above results show that zinc oxide is successfully combined with the hydrogel without changing the chemical structure of the hydrogel.

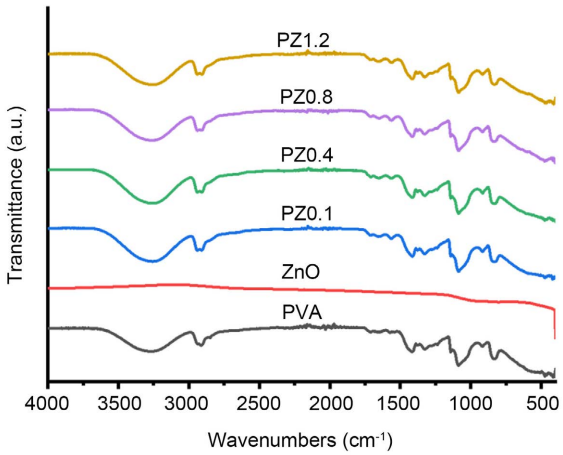

Figure 8. FTIR of zinc oxide PVA/ZnO conductive hydrogel with different mass percentages.

4) Tensile strength analysis

Figure 9 is the tensile strength analysis of hydrogels with different mass percentages of zinc oxide added. In the strength test analysis of hydrogels, due to the addition of different mass percentages of zinc oxide, the strength of the prepared hydrogels is somewhat different. It can be seen from the stress-strain curve that the strength of PVA/ZnO hydrogel first increases and then decreases. This is because, after the successful compounding of zinc oxide and polyvinyl alcohol, hydrogen bonding occurs between the two. The rigid structure of zinc oxide plays a scaffolding role in the three-dimensional system of the hydrogel, which improves the strength of the material. However, due to the combination of high-quality zinc oxide and polyvinyl alcohol, agglomeration will occur. This phenomenon hinders the polymerization of polyvinyl alcohol molecular chains and destroys the three-dimensional network system of the hydrogel, causing strength loss. Finally, based on the mechanical properties and strain properties of the material, a composite hydrogel is selected when the zinc oxide content is 0.1%. The hydrogel has the best mechanical properties, with a tensile strain of 296% and the ability to bear tensile stress. The tensile stress reaches 33.7 kPa, which is well-suitable for the field of flexible sensors.

5) Analysis of conductivity

In terms of electrochemical performance, it can be seen from Figure 10 that when the zinc oxide concentration is 0.1%, the electrical conductivity of the material is larger. This is because zinc oxide with a concentration of 0.1% can be evenly distributed in the PVA hydrogel, and is sufficient to provide adequate conductive paths. Therefore, this experiment uses a zinc oxide concentration of 0.1% as the sample for subsequent analysis and testing. When conducting conductivity tests on hydrogel samples with different zinc oxide concentrations, it was found that the highest conductivity reached 0.09 S/m with a zinc oxide con-

centration of 0.1%. This is because during the compounding process, due to the different concentrations of zinc oxide, it can be effectively dispersed in the system at low concentrations, does not affect the macromolecular chain of polyvinyl alcohol during compounding, and can effectively combine with free water in the system to achieve a stable increase in conductivity; in a high-concentration zinc oxide system, the zinc oxide content per unit volume in the system is too high, which may cause the agglomeration of macromolecular chains, which will lead to a decrease in the system's ability to bind free water. , seriously affecting the conductivity of hydrogel. Combining the mechanical properties and electrical conductivity of PZ conductive hydrogel, PZ0.1 is selected for further sensing performance testing.

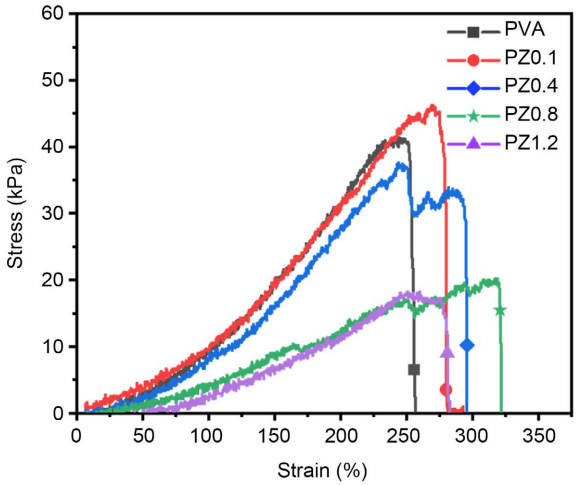

Figure 9. Stress-strain curves of PVA/ZnO conductive hydrogels with different mass percentages of zinc oxide.

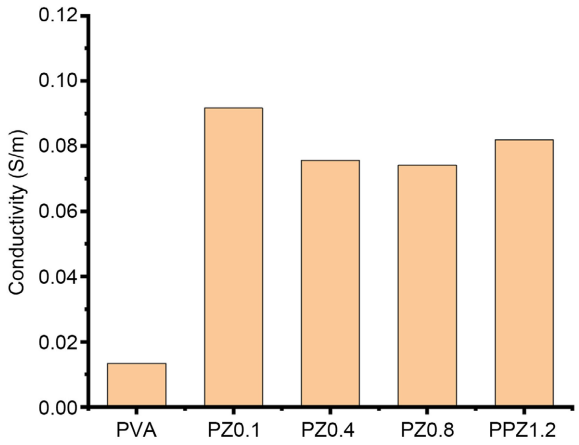

Figure 10. Conductivity of PVA/ZnO conductive hydrogels with different mass percentages of zinc oxide.

3.3. Characterization of Sensing Performance of PVA/ZnO Conductive Hydrogel

1) Tensile strain sensing

As shown in Figure 11, in the I-V curve of the material, the voltage ranges from −1 V to 1 V, and the material shows different I-V curve trends under different degrees of tensile strain. From the result analysis, it can be seen that the material is in the range of 0% - 70%. Under the tensile strain, the greater the tensile strain, the greater the slope of the curve, which means the greater the resistance of the hydrogel. During the stretching process under low strain, the microporous structure of the material deforms, causing the internal conductive paths to grow and the holes in the hydrogel to become smaller. The free water density decreases, resulting in an increase in the resistance of the material. During the subsequent strain process, the conductive path is borne by the solid structure of the hydrogel and the added zinc oxide, which increases the conductive properties of the material; after the strain gradually increases, the tensile strain of the material is carried by the macromolecular chains of the flexible PVA, whose conductive properties will cause changes in resistance due to the increase in conductive paths. During the gradual increase in strain, the conductive path changes from the original bound water to the conductive path of the internal zinc oxide material.

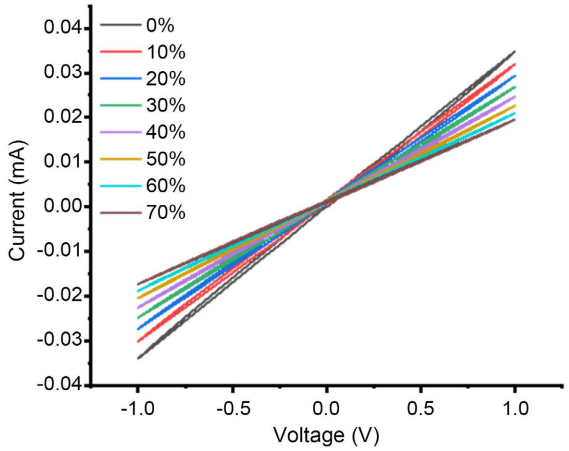

Figure 11. I-V curve of PZ0.1 conductive hydrogel.

In addition, the effect of different tensile strains on the resistance change rate of the conductive hydrogel at the same stretching speed is explored. From Figure 12, it can be seen that different tensile strains produce corresponding resistance change rates. When the strains are 2 mm, 4 mm, 6 mm, 8 mm, and 10 mm, respectively, they correspond to different resistance change rates, and there is a trend of gradient change, showing the changes in the electrical signal of the hydrogel sensor during the change process and the impact exerted by the hydrogel strain consistency. In the range of 0% - 50%, the relationship between $(R - R_0)/R_0$, strain, and time is shown in Figure 12. During the stretch release process, $(R - R_0)/R_0$ changes with the change of strain, so the $(R - R_0)/R_0$ value of the conductive hydrogel increases immediately during stretching, and the $(R - R_0)/R_0$ value the original value can be restored upon unloading, proving that the conductive hydrogel has good strain-sensing performance. Due to the excellent conductive network inside the hydrogel, the zinc oxide conductive network inside the hy-

drogel can effectively help the transfer of charges and accurately and effectively feedback the resistance changes in the composite film.

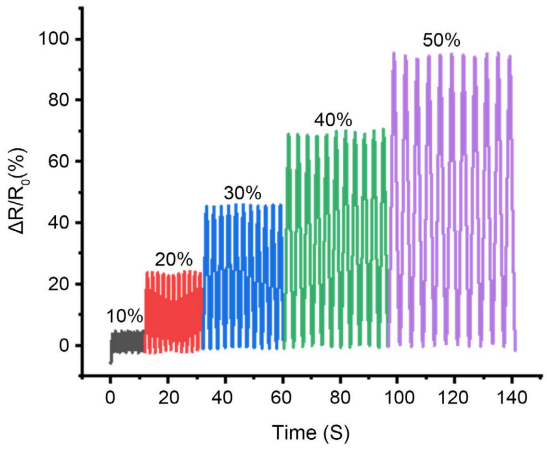

Figure 12. Test cycles of PZ0.1 conductive hydrogel under different tensile strains.

2) Stretch speed sensing

Figure 13 shows the cyclic stability and speed response effect of PZ0.1 conductive hydrogel under 20% strain. During the stretch release process, the $(R - R_0)/R_0$ change frequency is consistent with the strain change frequency, so the conductive hydrogel $(R - R_0)/R_0$ value gradually increases when stretched to 20%, the $(R - R_0)/R_0$ value returns to its original value during unloading, and the frequency of change is consistent with the rate of tensile strain. It can be seen from the figure that when the strains are the same and the stretching rates are 4 mm/s and 6 mm/s, respectively, the conductive hydrogel can maintain good strain-sensing stability, and the resistance change rate remains stable at 25%. Left and right, it is within the monitorable range and has an obvious speed response effect, which proves the unity of the electrical signal change of the hydrogel sensor and the frequency of the applied motion change and has a good speed response effect.

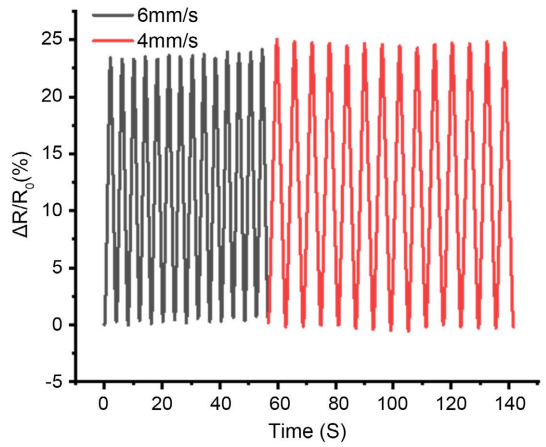

Figure 13. Test cycles of PZ0.1 conductive hydrogel under different rates of stretching.

3) Stretch sensitivity

Due to differences in the conductive mechanism of composite hydrogels, sensitivity fitting of the material is performed through the resistance change rate and the strain performance of the material during the tensile strain process to determine the strain response effect of hydrogel materials at different stages. The sensitivity coefficient (GF) is defined as the ratio of resistance change rate to strain. As shown in Figure 14, the gauge coefficient GF increases from 0% to 50% as the strain increases from 0% to 50%, indicating that the PVA/ZnO conductive hydrogel has high deformation sensitivity and excellent stretchability performance. The sensitivity factor shows that the conductive hydrogel's three-dimensional structure and zinc oxide's conductive mechanism can effectively respond positively to external strains. It shows that zinc oxide in the hydrogel system can improve the sensitivity and conductive properties of the material and make it applicable to a wider range.

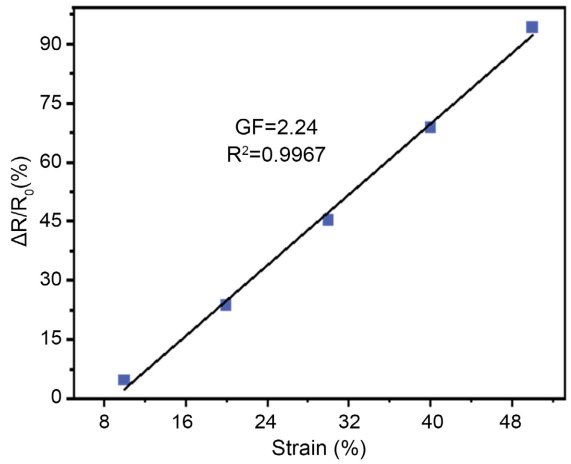

Figure 14. Tensile sensitivity fitting curve of PZ0.1 conductive hydrogel.

4) Response time

The response time and recovery time of conductive hydrogel sensors are important indicators for evaluating the sensing performance of conductive hydrogel sensors. The conductive hydrogel is maintained after being stretched to a small strain at a high stretching rate and then returns to its original position at the same rate. The response time and recovery time of the conductive hydrogel sensor are 700.85 ms and 711.36 ms, respectively, as shown in Figure 15. These results demonstrate that conductive hydrogels can quickly and accurately capture response signals under rapidly changing external motion stimuli.

5) Fatigue resistance

Flexible sensors for motion detection and the fatigue resistance of conductive hydrogels are particularly important. The key to the long-term use of sensor substrates is that the sensor material can maintain tensile fatigue resistance and maintain a stable resistance change rate after stretching cycles. The fatigue resis-

tance performance test is used to reflect the stability of the resistance change rate of the composite material under multiple cyclic stretchings. Under the strain condition of 40% strain stretching, a stretching cycle test is performed by a stepper motor. It can be seen from Figure 16 that in the fatigue resistance test of tensile cycles when the number of cycles gradually increases, the basic resistance of the hydrogel also gradually increases during the process. This is due to the gradual increase in resistance due to plastic deformation of the internal structure of the hydrogel during the fatigue resistance test process when the hydrogel is exposed to the air and loses moisture. It can be found that after multiple cycles, the resistance change rate of the conductive hydrogel stabilizes at 65%, indicating that the hydrogel has good self-recycling ability during the movement change process, which also benefits from the physical cross-linked network formed by hydrogen bonds. The tested performance of hydrogels in terms of fatigue resistance can maintain long-lasting stability, ensuring that hydrogels can be used in sensors.

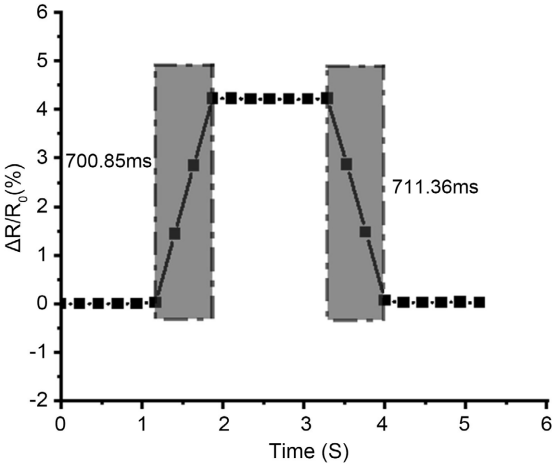

Figure 15. Stretch response time of PZ0.1 conductive hydrogel.

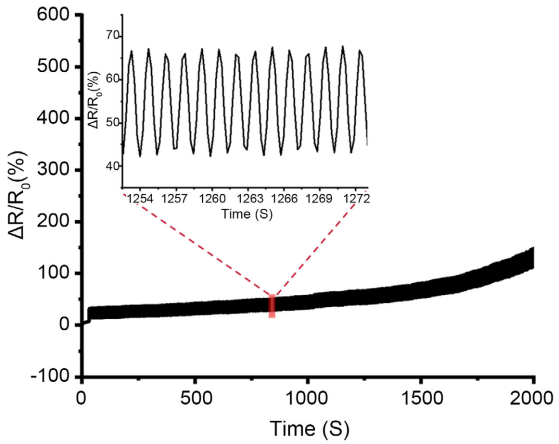

Figure 16. Fatigue resistance performance test of PZ0.1 conductive hydrogel.

Zinc oxide is introduced into PVA hydrogel to make PZ conductive hydrogel. The basic electron microscope morphology and chemical structure changes of the conductive hydrogel are tested and analyzed. The mechanical properties and conductivity changes are analyzed to determine the properties of zinc oxide. When the mass fraction is 0.1%, the material can maintain a good three-dimensional structure and electrical conductivity, and the electrical conductivity can reach 0.09 S/m. The maximum tensile strain of the material can reach 296%, and the tensile stress is 33.7 kPa. Through the tensile strain sensing performance test of the material, the tensile sensing application of the material is explored and analyzed. The speed-sensing effect of strain at 20% is significant. The strain sensitivity of the material at 50% is determined to be 2.24. In terms of stretch response, the response time and recovery time reach 700.85 ms and 711.36 ms, respectively. The fatigue resistance of the material can also reach about 800 times, and it can monitor and identify motion signals from different parts of the human body. It is a sensor material with good performance.

3.4. Application of PVA/ZnO Conductive Hydrogel in Flexible Sensors

The zinc oxide within the composite hydrogel provides the material with good electrical conductivity. In the study, zinc oxide is combined with a PVA hydrogel matrix to provide a conductive matrix for the composite hydrogel, and a conductive hydrogel system with excellent mechanical and electrical properties is prepared as a substrate for a stretch sensor. In order to test the motion-sensing effect of the material, the composite hydrogel is applied to twists, fingers, wrists, knees, etc. as stretch sensors for human body motion monitoring. In actual motion monitoring, the material can effectively feedback on the movement changes of the human body and has good electrical signal output effects for different degrees of motion, confirming the feasibility of the material being used in flexible sensors.

1) Sports monitoring

Figure 17 shows the feedback effect of the composite hydrogel on the bending angle of the finger. The resistance change rate of the material changes when the finger is bent and extended to different angles. The conductive hydrogel is stretched when the fingers are bent to different angles, and the material's resistance recovers during the bending recovery motion. When the bending angle is constant, the material can maintain resistance stability within a corresponding period of time and maintain the resistance change characteristics of the material during the bending process. When the bending angle gradient changes, the material resistance also undergoes a gradient change trend, indicating that the conductive hydrogel composite material has high sensitivity and can be used to monitor and distinguish different movements of the index finger. When the finger is bent to a certain angle and remains motionless, the relative current change of the sensor increases to a specific value and remains stable. If the finger con-

tinues to be bent, the resistance change rate of the sensor continues to increase, showing a stepwise upward trend. There are different degrees of resistance change rates when bending to 30˚, 60˚, 90˚, and 120˚, respectively, and the same stability can be maintained at the end of bending, which shows that the monitoring effect of hydrogel materials on finger bending is repeatable, which can be applied to joint movements of the human body.

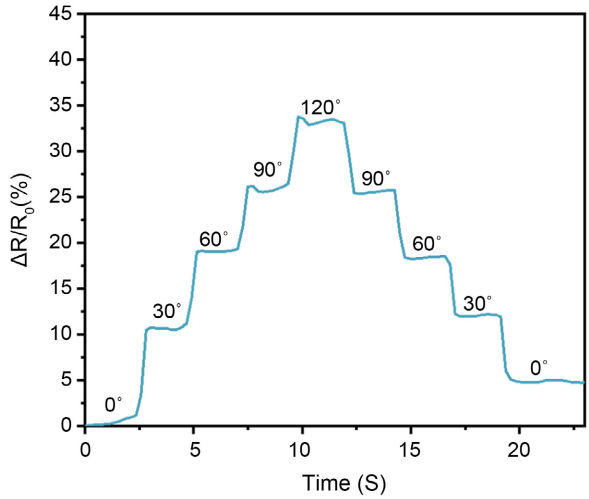

Figure 17. Finger bending strain sensing performance of PZ0.1 conductive hydrogel.

Figure 18 shows the resistance change reflected by the bending speed of the conductive hydrogel material. Since the deformation speed of the deformed material during the bending process is different, it can be found that the material maintains stability during deformation at different bending speeds and can return to the initial strain resistance position. Moreover, the signal frequency of the conductive hydrogel changes significantly at different bending speeds, indicating that the material can be effectively used to monitor speed deformation.

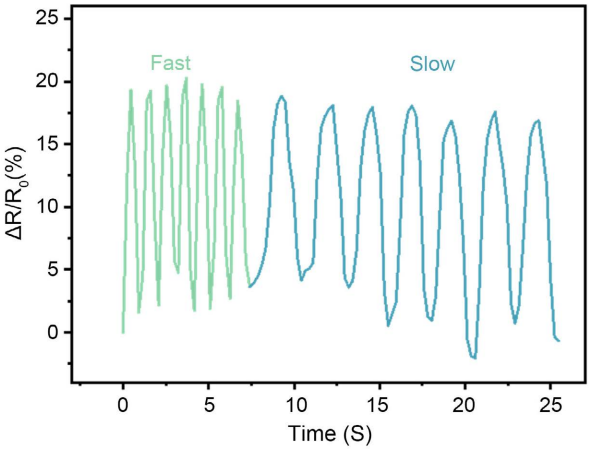

Figure 18. Finger bending fast and slow strain sensing performance of PZ0.1 conductive hydrogel.

Figure 19 shows the resistance change reflected by the conductive hydrogel material in response to finger bending. Since the deformed material deforms to different degrees during the bending process, it can be found that the material maintains stability during different bending deformations and can return to the initial strain resistance position. Moreover, the signal frequency of the conductive hydrogel changes significantly under different degrees of bending, indicating that the material can be effectively used to monitor different deformations.

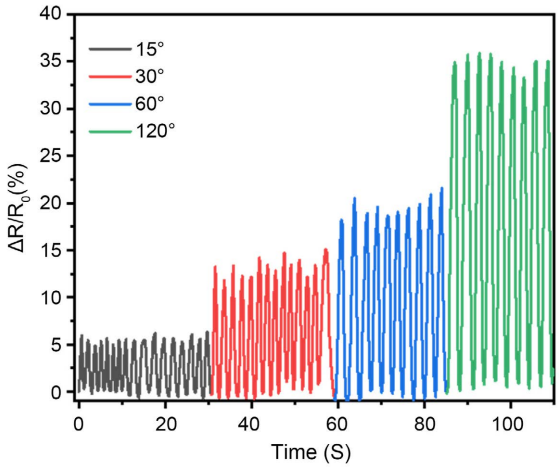

Figure 19. Repeated experiments on finger bending strain of PZ0.1 conductive hydrogel.

Figure 20 shows the resistance change reflected by the conductive hydrogel material in response to bending and torsion. Due to the extrusion deformation of the deformed part of the material during the torsion process, the width of the conductive path is reduced and the resistance is increased. It can be found that the material maintains stability during torsional deformation and can return to the initial strain resistance position. This shows that the material can be effectively used to monitor torsional deformation.

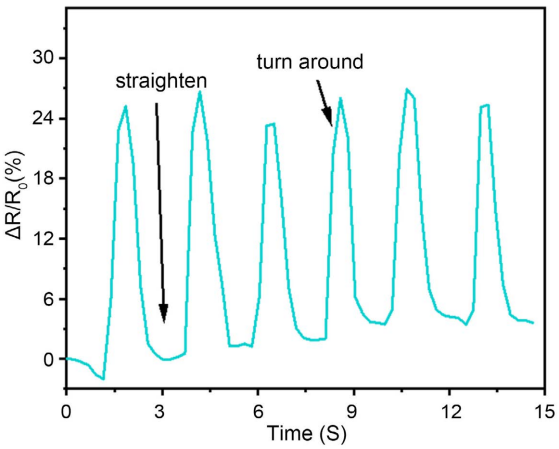

Figure 20. Torsional deformation sensing performance of PZ0.1 conductive hydrogel.

As shown in Figure 21, when the hydrogel material is attached to the fingers, cheeks, neck, knees, wrists, and ankles for motion monitoring, it can be found that the monitoring of different parts has different resistance change rates and can be used cyclically to monitor various parts.

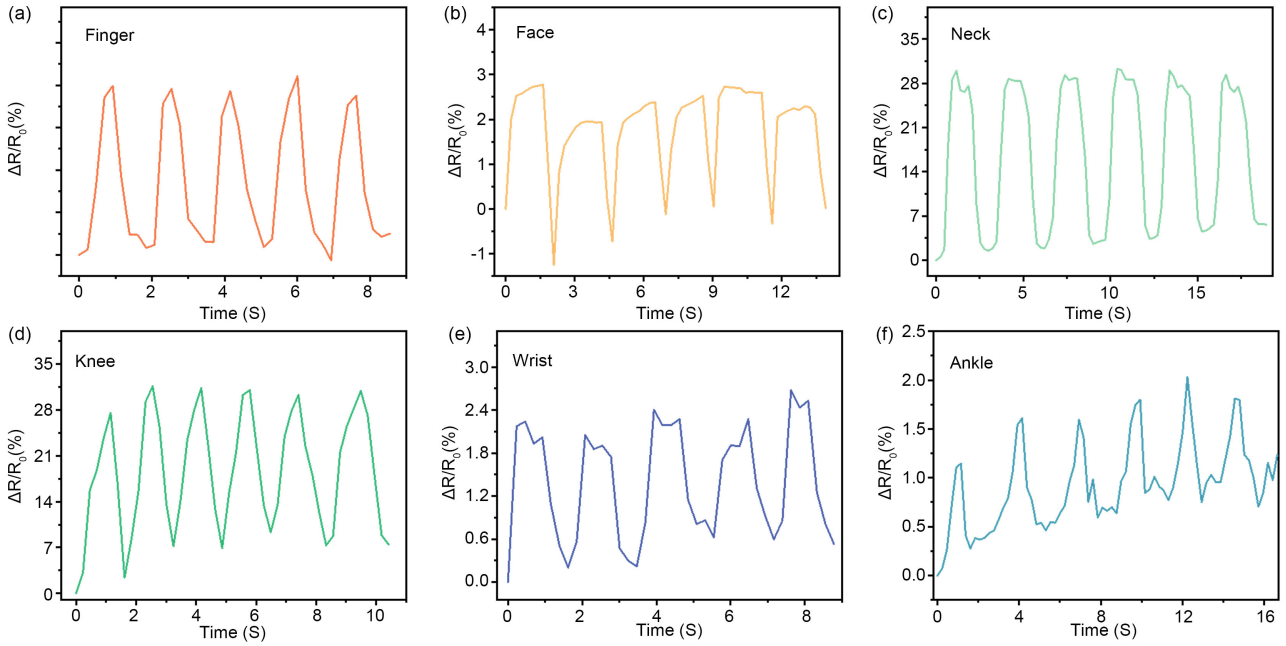

Figure 21. PZ0.1 conductive hydrogel motion signal monitoring.

By monitoring human activities, we can find that resistive composite hydrogel sensors prepared with conductive hydrogel substrates can effectively distinguish the intensity and frequency of human movement by using the strain sensitivity of the material.

4. Conclusion

In this study, a hydrogel motion sensor with excellent performance is prepared by modifying hydrogel materials. In terms of sensor sensitivity, they can achieve a high response speed and provide corresponding electrical signal changes in a timely and accurate manner. The mechanical properties of the material and related sensing effect tests provide guidance for the use of polyvinyl alcohol composites in flexible conductive hydrogels. Based on the ionic hydrogel, PANI serves as the structural support of the material and the three-dimensional conductive network inside the material to improve the stress performance and conductive performance of the material in terms of sensors. After the rigid molecular chains of polyaniline are introduced, the micromorphology and structure of the material change, which are analyzed and confirmed by FE-SEM, FTIR, and XRD. After finally passing the mechanical properties and conductivity analysis and testing, combined with the best performance parameters of the required sensor, the optimal mass fraction of zinc oxide is 0.1%. The electrical conductivity of PZ conductive hydrogel can reach up to 0.09 S/m; PZ conductive hydrogel

has good tensile strain performance (50%), sensitive response speed (700.85 ms), and good stability (800 times). It is a sensor material with good performance. The sensor can be effectively used in human body motion monitoring. In terms of monitoring the movement of finger joints, it can not only provide feedback on the frequency of movement of the knuckles but also intuitively reflect the angle of knuckle bending. This shows that the movement sensitivity of the sensor is also suitable for monitoring such movement changes as elbows and knees, etc. Large-scale movements of moving joints can also achieve accurate monitoring results. This is due to the wide monitoring range of the prepared hydrogel substrate and is also related to the size of the recoverable strain carried by the hydrogel.

Conflicts of Interest

The authors declare no conflicts of interest regarding the publication of this paper.

References

[1] Ge, G., Lu, Y., Qu, X., *et al.* (2020) Muscle-Inspired Self-Healing Hydrogels for Strain and Temperature Sensor. *ACS Nano*, **14**, 218-228. https://doi.org/10.1021/acsnano.9b07874

[2] Huang, J., Zeng, J., Zhang, X., *et al.* (2022) Fatigue Resistant Aerogel/Hydrogel Nanostructured Hybrid for Highly Sensitive and Ultrabroad Pressure Sensing. *Small*, **18**, Article ID: 2104706. https://doi.org/10.1002/smll.202104706

[3] Zafer, A. and Yadav, S. (2018) Design and Development of Strain Gauge Pressure Transducer Working in High Pressure Range of 500 MPa Using Autofrettage and Finite Element Method. *International Journal of Precision Engineering and Manufacturing*, **19**, 793-800. https://doi.org/10.1007/s12541-018-0095-y

[4] Jia, L., Zhou, C., Dai, K., *et al.* (2022) Facile Fabrication of Highly Durable Superhydrophobic Strain Sensors for Subtle Human Motion Detection. *Journal of Materials Science & Technology*, **110**, 35-42. https://doi.org/10.1016/j.jmst.2021.08.081

[5] Ju, M., Wu, B., Sun, S., *et al.* (2020) Redox-Active Iron-Citrate Complex Regulated Robust Coating-Free Hydrogel Microfiber Net with High Environmental Tolerance and Sensitivity. *Advanced Functional Materials*, **30**, Article ID: 1910387. https://doi.org/10.1002/adfm.201910387

[6] Eder, C., Valente, V., Donaldsn, N., *et al.* (2014) A CMOS Smart Temperature and Humidity Sensor with Combined Readout. *Sensors*, **14**, 17192-17211. https://doi.org/10.3390/s140917192

[7] Zang, Y., Zhang, F., Di, C.A., *et al.* (2014) Advances of Flexible Pressure Sensors toward Artificial Intelligence and Health Care Applications. *Materials Horizons*, **2**, 140-156. https://doi.org/10.1039/C4MH00147H

[8] Lu, Y., Qu, X., Wang, S., *et al.* (2022) Ultradurable, Freeze-Resistant, and Healable MXene-Based Ionic Gels for Multi-Functional Electronic Skin. *Nano Research*, **15**, 4421-4430. https://doi.org/10.1007/s12274-021-4032-5

[9] Daisuke, Y., Shogo, N., Kenichiro, K., *et al.* (2017) A Planar, Multisensing Wearable Health Monitoring Device Integrated with Acceleration, Temperature, and Electrocardiogram Sensors. *Advanced Materials Technologies*, **2**, Article ID: 1700057. https://doi.org/10.1002/admt.201700057

[10] Tan, C., Dong, Z., Li, Y., *et al.* (2020) A High Performance Wearable Strain Sensor with Advanced Thermal Management for Motion Monitoring. *Nature Communications*, **11**, Article No. 3530. https://doi.org/10.1038/s41467-020-17301-6

[11] Zhang, Y., Fang, Y., Li, J., *et al.* (2017) Dual-Mode Electronic Skin with Integrated Tactile Sensing and Visualized Injury Warning. *ACS Applied Materials & Interfaces*, **9**, 37493–37500. https://doi.org/10.1021/acsami.7b13016

[12] Chortos, A., Liu, J. and Bao, Z. (2016) Pursuing Prosthetic Electronic Skin. *Nature Materials*, **15**, 937-950. https://doi.org/10.1038/nmat4671

[13] Araki, T., Uemura, T., Yoshimoto, S., *et al.* (2020) Wireless Monitoring Using a Stretchable and Transparent Sensor Sheet Containing Metal Nanowires. *Advanced Materials*, **32**, Article ID: 1902684. https://doi.org/10.1002/adma.201902684

[14] Xu, B., Akhtar, A., Liu, Y., *et al.* (2016) An Epidermal Stimulation and Sensing Platform for Sensorimotor Prosthetic Control, Management of Lower Back Exertion, and Electrical Muscle Activation. *Advanced Materials*, **28**, 4462-4471. https://doi.org/10.1002/adma.201504155

[15] Zhang, D., Zhou, W., Wei, B., *et al.* (2015) Carboxyl-Modified Poly (Vinyl Alcohol)-Crosslinked Chitosan Hydrogel Films for Potential Wound Dressing. *Carbohydrate Polymers*, **125**, 189-199. https://doi.org/10.1016/j.carbpol.2015.02.034

[16] Wen, N., Jiang, B.J., Wang, X.J., *et al.* (2020) Overview of Polyvinyl Alcohol Nanocomposite Hydrogels for Electro-Skin, Actuator, Supercapacitor and Fuel Cell. *The Chemical Record*, **20**, 773-792. https://doi.org/10.1002/tcr.202000001

[17] Wu, L.J., Huang, S.Q., Zheng, J., *et al.* (2019) Synthesis and Characterization of Biomass Lignin-Based PVA Super-Absorbent Hydrogel. *International Journal of Biological Macromolecules*, **140**, 538-545. https://doi.org/10.1016/j.ijbiomac.2019.08.142

[18] Montaser, A.S., Rehan, M. and El-Naggar, M.E. (2019) PH-Thermosensitive Hydrogel Based on Polyvinyl Alcohol/Sodium Alginate/N-Isopropyl Acrylamide Composite for Treating Re-Infected Wounds. *International Journal of Biological Macromolecules*, **124**, 1016-1024. https://doi.org/10.1016/j.ijbiomac.2018.11.252

[19] Sahu, D., Sarkar, N., Sahoo, G., *et al.* (2017) Nano Silver Imprinted Polyvinyl Alcohol Nanocomposite Thin Films for Hg^{2+} Sensor. *Sensors and Actuators B*: *Chemical*, **246**, 96-107. https://doi.org/10.1016/j.snb.2017.01.038

[20] Xiao, D. (2019) Preparation and Application of Nano-Zinc Oxide. *Contemporary Chemical Engineering Research*, **10**, 168-169.

[21] Abdullah, F.H., Abu Bakar, N.H.H. and Abu Bakar, M. (2022) Current Advancements on the Fabrication, Modification, and Industrial Application of Zinc Oxide as Photocatalyst in the Removal of Organic and Inorganic Contaminants in Aquatic Systems. *Journal of Hazardous Materials*, **424**, Article ID: 127416. https://doi.org/10.1016/j.jhazmat.2021.127416

[22] Hu, Z.J., Zhao, Z. and Wang, X.M. (2012) Antibacterial Properties and Mechanism of Nano-Zinc Oxide. *Chinese Tissue Engineering Research*, **16**, 527-530.

[23] Yamamoto, O., Nakakoshi, K., Sasamoto, T., *et al.* (2001) Adsorption and Growth Inhibition of Bacteria on Carbon Materials Containing Zinc Oxide. *Carbon*, **39**, 1643-1651. https://doi.org/10.1016/S0008-6223(00)00289-X

[24] Chen, N.L., Feng, H.X., Wang, Y., *et al.* (2009) Research Progress of Nanometer Silver-Loaded Inorganic Antibacterial Agents. *Applied Chemical Engineering*, **38**, 717-720.

[25] Salama, A. (2018) Chitosan/Silk Fibroin/Zinc Oxide Nanocomposite as a Sustaina-

ble and Antimicrobial Biomaterial. *Cellulose Chemistry and Technology*, **52**, 903-907.

[26] Tofa, T.S., Kunjali, K.L., Paul, S. and Dutta, J. (2019) Visible Light Photocatalytic Degradation of Microplastic Residues with Zinc Oxide Nanorods. *Environmental Chemistry Letters*, **17**, 1341-1346. https://doi.org/10.1007/s10311-019-00859-z

[27] Zhao, W.F., Wang, C.S., Zhang, M., *et al.* (2020) Application of Nano-Zinc Oxide in Areca Nut Cellulose Short Fiber/Natural Rubber Composite Materials. *Rubber Industry*, **67**, 843-846.

[28] Zhang, B., Liang, T., Shao, X., *et al.* (2021) Nondestructive Grafting of ZnO on the Surface of Aramid Fibers Followed by Silane Grafting to Improve Its Interfacial Adhesion Property with Rubber. *ACS Applied Polymer Materials*, **3**, 4587-4594. https://doi.org/10.1021/acsapm.1c00682

[29] Liu, Y.Y. and Xiong, Y. (2021) Research Progress of Nano Zinc Oxide Sensors. *Semiconductor Technology*, **46**, 1-10.

[30] Malara, A., Bonaccorsi, L., Donato, A., *et al.* (2019) Doped Zinc Oxide Sensors for Hexanal Detection. In: Di Francia, G., *et al.* Eds., *AISEM* 2019: *Sensors and Microsystems*, Springer, Cham, 279-285. https://doi.org/10.1007/978-3-030-37558-4_42

[31] Wood, G.S., Jeronimo, K., Mahzan, M., *et al.* (2021) Zinc Oxide Nanowires-Based Flexible Pressure Sensor. *Micro & Nano Letters*, **16**, 432-435. https://doi.org/10.1049/mna2.12069

[32] Van Vlierberghe, S., Dubruel, P. and Schacht, E. (2011) Biopolymer-Based Hydrogels as Scaffolds for Tissue Engineering Applications: A Review. *Biomacromolecules*, **12**, 1387-1408. https://doi.org/10.1021/bm200083n

[33] Jiang, X.C., Xiang, N.P., Zhang, H.X., *et al.* (2018) Preparation and Characterization of Poly (Vinyl Alcohol)/Sodium Alginate Hydrogel with High Toughness and Electric Conductivity. *Carbohydrate Polymers*, **186**, 377-383. https://doi.org/10.1016/j.carbpol.2018.01.061

[34] Mao, J., Zhao, C., Li, Y., *et al.* (2020) Highly Stretchable, Self-Healing, and Strain-Sensitive Based on Double-Crosslinked Nanocomposite Hydrogel. *Composites Communications*, **17**, 22-27. https://doi.org/10.1016/j.coco.2019.10.007

[35] Zhang, Y., El Demellawi Jehad, K., Jiang, Q., *et al.* (2020) MXene Hydrogels: Fundamentals and Applications. *Chemical Society Reviews*, **49**, 7229-7251. https://doi.org/10.1039/D0CS00022A

[36] Debasis, M., Krishnamoorthy, R. and Ramasamy, T.R.K. (2018) Polyvinyl Alcohol Wrapped Multiwall Carbon Nanotube (MWCNTs) Network on Fabrics for Wearable Room Temperature Ethanol Sensor. *Sensors and Actuators B*: *Chemical*, **261**, 297-306. https://doi.org/10.1016/j.snb.2018.01.152

[37] Ma, Z., Shi, W., Ke, Y., *et al.* (2019) Doping Engineering of Conductive Polymer Hydrogels and Their Application in Advanced Sensor Technologies. *Chemical Science*, **10**, 6232-6244. https://doi.org/10.1039/C9SC02033K

[38] Zhang, Y.F. (2022) Controllable Preparation of MXene Nanocomposite Hydrogel and Research on Its Wearable Smart Medical Diagnosis and Treatment Performance. Ph.D. Thesis, Beijing University of Chemical Technology, Beijing.

[39] He, P., Wu, J., Pan, X., *et al.* (2020) Anti-Freezing and Moisturizing Conductive Hydrogels for Strain Sensing and Moist-Electric Generation Applications. *Journal of Materials Chemistry A*, **8**, 3109-3118. https://doi.org/10.1039/C9TA12940E

[40] Ali, N., Harpinder, S., Wayne, C., *et al.* (2016) Gold Nanorod-Incorporated Gelatin-Based Conductive Hydrogels for Engineering Cardiac Tissue Constructs. *Acta Biomaterialia*, **41**, 133-146. https://doi.org/10.1016/j.actbio.2016.05.027

[41] Singhal, U., Khanuja, M., Prasad, R. and Varma, A. (2017) Impact of Synergistic Association of ZnO-Nanorods and Symbiotic Fungus Piriformospora Indica DSM 11827 on Brassica Oleracea var. Botrytis (Broccoli). *Frontiers in Microbiology*, **8**, Article 1909. https://doi.org/10.3389/fmicb.2017.01909